

H_∞ control design with feed-forward compensator for hysteresis compensation in piezoelectric actuators

DOI 10.7305/automatika.2017.02.1786
UDK 681.532.8.073-022.513:[681.587.09-55:539.389.4]

Original scientific paper

Piezoelectric actuators, widely used in different micro/nanopositioning applications, generally exhibit nonlinear hysteresis characteristics. The compensation of hysteretic behavior of piezoelectric actuators is mandatory for precise micro/nanopositioning. In this paper, nonlinear hysteresis effect is first characterized using the Prandtl-Ishlinskii hysteresis model. The inverse of the Prandtl-Ishlinskii hysteresis model is employed as a feed-forward controller to compensate for hysteresis nonlinearities of the piezoelectric actuator. Slight hysteresis nonlinearity is still observed in the experimental results due to small mismatch between the identified hysteresis model and the measured hysteresis loop. To further enhance the performance of the piezoelectric actuator in terms of mitigation of hysteresis nonlinearity and precise reference tracking, advanced robust full-order as well as fixed-order H_∞ feedback controllers are designed and applied to this actuator in the presence of feed-forward compensator. The experimental results verify the effectiveness of the proposed control scheme in achieving the improved tracking performance with peak-to-peak tracking error of less than 1% for the desired displacement of 12 μm with tracking frequency of 10 Hz.

Key words: Feed-forward compensator, Full-order and fixed-order H_∞ feedback controllers, Piezoelectric actuator, Prandtl-Ishlinskii hysteresis model

Sinteza H_∞ regulatora s unaprijednom granom za kompenzaciju histereze kod piezoelektričnih aktuatora. Piezoelektrični aktuatori, rasprostranjeni u različitim primjenama mikro/nanopozicioniranja, općenito su izloženi nelinearnim histereznim karakteristikama. Kompenzacija histereznog ponašanja piezoelektričnih aktuatora nužna je za precizno mikro/nanopozicioniranje. Inverzni Prandtl-Ishlinskii histerezni model korišten je za unaprijednu kompenzaciju histereznih nelinearnosti piezoelektričnog aktuatora. Neznatna histerezna nelinearnost još uvijek je vidljiva u eksperimentalnim rezultatima zbog malog neslaganja između identificiranog histereznog modela i mjerene histerezne petlje. Za daljnje poboljšanje performansi piezoelektričnog aktuatora u smislu smanjenja histerezne nelinearnosti i preciznog slijeđenja reference, napredni robusni H_∞ regulatori punog i određenog reda sintetizirani su i primijenjeni na ovaj aktuator uz prisutnost unaprijednog kompenzatora. Eksperimentalni rezultati potvrđuju efektivnost predložene upravljačke strukture u postizanju poboljšanih performansi slijeđenja, uz vršnu vrijednost pogreške manju od 1% za ciljani pomak od 12 μm s frekvencijom slijeđenja od 10 Hz.

Ključne riječi: Unaprijedni kompenzator, H_∞ regulator punog i određenog reda, piezoelektrični aktuator, Prandtl-Ishlinskii histerezni model

1 INTRODUCTION

Micro/nanopositioning is an important aspect of research in micro/nanotechnology where ultrahigh positioning precision is one of the pivotal requirements. Piezoelectric actuators are widely used in different micro/nanopositioning [1] and atomic-scale surface scanning applications [2]. However, the positioning precision of these actuators can be significantly reduced due to nonlinear hysteresis effects when they are used in relatively long range positioning applications [3]. Nonlinear hysteresis effects, if not compensated, can cause inaccuracy and

oscillations in the system response, and could also lead to instability of the closed loop system [4].

A number of hysteresis models have been developed [5] in order to facilitate the design of controllers for compensating its effects. Some of these models are Bouc-Wen model [6], Duhem model [7], Jiles-Atherton model [8], Preisach model [9], Krasnosel'skii-Pokrovskii model [10], Prandtl-Ishlinskii model [11], Maxwell-based model [12] etc. The most commonly used operator based hysteresis models are Preisach model and Prandtl-Ishlinskii model. The advantage of Prandtl-Ishlinskii model over Preisach

model is that its inverse can be attained analytically which can be implemented as a feed-forward controller to compensate hysteresis effects [13]. This makes the Prandtl-Ishlinskii model convenient for different real-time micro/nanopositioning applications [14].

Generally, there are two control approaches commonly adopted in the literature to compensate the hysteresis effects. The first approach is inverse-based hysteresis compensation in open-loop, where inverse hysteresis model is cascaded with hysteresis model to compensate the nonlinear hysteresis effects. This approach requires formulation of inverse hysteresis model which is often a challenging task [14]. Also, if there is any small mismatch between the output of the hysteresis model and the measured hysteresis loop then the inverse hysteresis model will not be able to compensate the hysteretic behavior effectively. The second approach is model-based hysteresis compensation, where different feedback controllers are designed to compensate hysteresis effects, without employing the inverse hysteresis model. Different kind of control algorithms like hybrid control [15], robust control [16, 17], adaptive control [18, 19] and classical PID (proportional-integral-derivative) control [20] have been investigated in the literature for compensating the hysteresis effects. Other than these two approaches, it has also been discussed in the literature that the nonlinear hysteresis effects can also be compensated by actuating the piezoelectric actuators using charge amplifiers (rather than voltage amplifiers) [21]. However, in spite of its benefits, the charge actuation has not been generally accepted due to the practical problems of voltage drift, poor low frequency response and also commercially unavailability of the charge sources [22].

In order to compensate nonlinear hysteresis effects for precise micro/nanopositioning, a combination of feed-forward and feedback controllers is also recently investigated in the literature. In [23], the observer-based inverse hysteresis approach in parallel combination with classical linear proportional-integral (PI) feedback controller is proposed for hysteresis compensation in magnetic shape memory actuators. In [24], an inverse Prandtl-Ishlinskii hysteresis model-based compensator combined with linear proportional-integral (PI) feedback controller is applied to piezoelectric actuator in order to compensate for hysteresis nonlinearities. In [25], inverse Maxwell resistive capacitor model is used as a feed-forward compensator in order to achieve a linearized system with hysteresis compensation. Then, a classical proportional-integral (PI) feedback controller is designed for linearized system in order to improve the tracking performance of piezoelectric actuator. The combination of feed-forward and feedback controllers is also discussed in literature for the compensation of hysteresis as well as structural vibrations. In [26], a proportional-derivative (PD) high-gain feedback

controller is proposed to linearize the hysteresis nonlinearity of piezoelectric actuator. With this feedback controller, an optimal inversion approach of linear vibrational dynamics is also adopted to design the feed-forward inputs in order to compensate the induced structural vibrations during high speed positioning. In all these papers, classical (PI / PD) controller is implemented as feedback controller with a feed-forward compensator. Advanced H_∞ feedback controller is also widely used without any feed-forward compensator in different nanopositioning and atomic scale surface scanning applications [27–30]. The main contribution of this paper is to analyze the performance of the considered piezoelectric actuator system with advanced robust full-order as well as fixed-order H_∞ feedback controllers in the presence of inverse Prandtl-Ishlinskii hysteresis model, used as a feed-forward compensator, in order to achieve enhanced reference tracking performance with the compensation of hysteresis effects. Experimental results are provided to demonstrate the effectiveness of the proposed control scheme.

The working principle with complete description of the considered experimental setup is given in Section 2. The system modeling for controller design and system identification is provided in Section 3. Section 4 then presents full-order as well as fixed-order H_∞ controllers design and its performance analysis. Experimental results to analyze the performance of feed-forward/feedback controllers are presented in Section 5. Finally, Section 6 draws some conclusions.

2 SYSTEM DESCRIPTION

In this section, the working principle of the considered system and experimental details will be presented.

2.1 Working principle

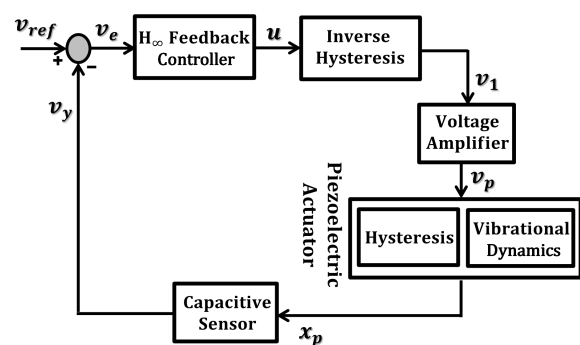


Fig. 1. Closed-loop control scheme of considered system

A complete closed-loop control scheme which will be considered here is presented in Fig. 1. Piezoelectric actuator is used here for precise micro/nanopositioning which

has vibrational dynamics as well as the nonlinear hysteresis characteristics. Inverse hysteresis model is proposed here as a feed-forward compensator to mitigate hysteresis effects of the piezoelectric actuator. A voltage amplifier is used before piezoelectric actuator at the output of the feed-forward compensator. The displacement (x_p) of the piezoelectric actuator is sensed by a capacitive sensor. The reference voltage corresponds to the desired displacement of the piezoelectric actuator. Any variation in the desired displacement will generate the error voltage (v_e). Then, feedback controller will take necessary action and generates an output voltage (u) available for feed-forward compensator. The objective of control design here is to achieve precise reference tracking with robustness and stability.

2.2 Experimental details

The block diagram of experimental setup used for real-time experimentation is presented in Fig. 2. The actual experimental setup is also presented here in Fig. 3. The setup consists of a single axis piezoelectric nanopositioning stage (P-752.21) driven by a high-power piezo amplifier (E-505.00). The nanopositioning stage has input voltage range from 0-100 V and provides a positioning and scanning range up to 35 μm . The resonant frequency of this stage is 2100 Hz with a resolution of 0.2 nm. The piezo amplifier has input voltage range of -2 to +12 V with a voltage gain of 10 V. The amplifier receives the control signal from the computer, having LabVIEW software, through data acquisition card (NI PXIe-6361). A capacitive position sensor (D-015) is used to measure the displacement of the nanopositioning stage. This sensor has nominal measurement range of 15 μm with a resolution of 0.01 nm. The capacitive position sensors are widely used in nanopositioning as they provide non-contact measurements with sub-nanometer resolution and high bandwidth. The output of the capacitive sensor is given back to the computer through data acquisition card as shown in Fig. 2.

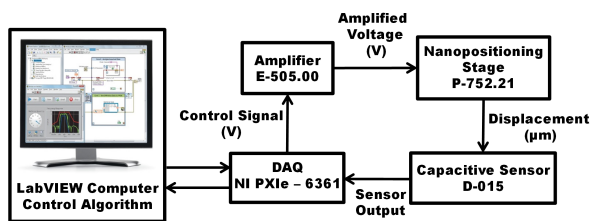


Fig. 2. Block diagram of experimental loop

3 DYNAMIC MODELING AND SYSTEM IDENTIFICATION

In this section, the mathematical model of the considered nanopositioning system as well as system identifica-

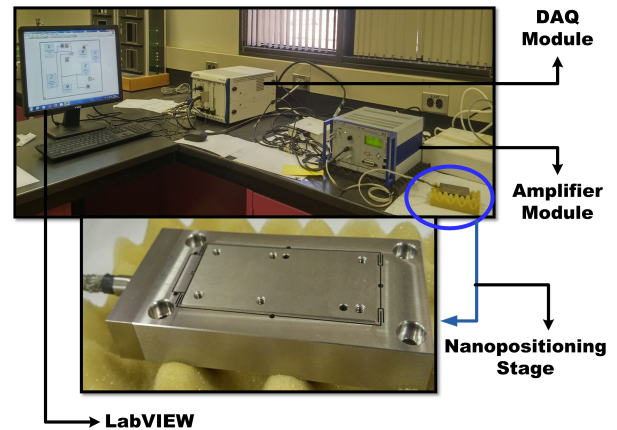


Fig. 3. Experimental setup in lab

tion of linear dynamics and nonlinear hysteresis characteristics will be presented.

3.1 Linear dynamics

The linear part of considered nanopositioning system consists of a voltage amplifier, vibrational dynamics of piezoelectric actuator and a capacitive position sensor.

The voltage amplifier is modeled by a first order transfer function as:

$$\frac{V_p(s)}{V_1(s)} = \frac{G_v \omega_v}{s + \omega_v}, \quad (1)$$

where V_1 and V_p are the input and output voltages of the voltage amplifier respectively, ω_v is the bandwidth and G_v the gain of the amplifier. The vibrational dynamics of the piezoelectric actuator is modeled by a second order transfer function as:

$$G_{vib}(s) = \frac{G_a \omega_a^2}{s^2 + 2\zeta \omega_a s + \omega_a^2}, \quad (2)$$

where ζ is the damping, ω_a the bandwidth and G_a the gain of the piezoelectric actuator. The capacitive position sensor dynamics is modeled by a first order transfer function as:

$$\frac{V_y(s)}{X_p(s)} = \frac{G_c \omega_c}{s + \omega_c}, \quad (3)$$

where X_p and V_y are the input displacement and output voltage of the capacitive sensor respectively, ω_c is the bandwidth and G_c the gain of the sensor.

So, the linear dynamics of the considered nanopositioning system can be represented by the fourth order transfer function and the identification of this transfer function will be presented in the Subsection 3.4.

3.2 Prandtl-Ishlinskii hysteresis model

In this section, the Prandtl-Ishlinskii hysteresis model [13] is presented by using symmetric generalized play operators to model the nonlinear hysteresis of the piezoelectric actuator. The play operator, characterized by the input v_p and the threshold r , determines the width of the hysteresis operator. The output of the generalized play operator $H_r[v_p](t)$ for any input $v_p(t)$ is defined as follows:

$$\begin{aligned} \Phi(0) &= H_r[v_p](0) = h_r(v_p(0), (0)), \\ \Phi(t) &= H_r[v_p](t) = h_r(v_p(t), H_r[v_p](t - T)), \quad (4) \\ h_r(v_p, \Phi) &= \max(\gamma(v_p) - r, \min(\gamma(v_p) + r, \Phi)), \end{aligned}$$

where r refers to the threshold which is the magnitude of increasing or decreasing input v_p corresponding to zero output Φ and γ is an envelope function. A linear envelop function $\gamma(v_p) = c_0 \cdot v_p(t) + c_1$ is considered here to model the symmetric hysteresis properties of the piezoelectric actuator where c_0 and c_1 are constant parameters whose values are identified from the experimental data.

The Prandtl-Ishlinskii hysteresis model is formulated by using symmetric generalized play operator $\Phi(t)$ to yield output $F[v_p](t)$ as:

$$x_p(t) = F[v_p](t) = \alpha \gamma(v_p(t)) + \sum_{j=1}^n g_j H_{r_j}[v_p](t), \quad (5)$$

where n is the number of generalized play operators, g is corresponding weight and α is a positive constant. For the considered piezoelectric actuator, the threshold values and the weights are chosen as $r_j = \beta \cdot j$ and $g_j = \rho \cdot \exp(-\tau \cdot r_j)$ for $j = 1, 2, 3, \dots, n$ where β, ρ, τ and n are positive constants whose values are identified from the real-time experimental data.

3.3 Inverse Prandtl-Ishlinskii hysteresis model

In this section, analytical inverse of the Prandtl-Ishlinskii hysteresis model is presented for the purpose of using it as a feed-forward compensator to mitigate nonlinear hysteresis of the piezoelectric actuator. The threshold (q) of the inverse model is related to the threshold (r) of the Prandtl-Ishlinskii hysteresis model as:

$$q_j = \alpha \cdot r_j + \sum_{i=1}^{j-1} g_i (r_j - r_i), \quad (6)$$

where α is a positive constant and g is a weighting function of the Prandtl-Ishlinskii hysteresis model. The weighting function (p) of the inverse model is given by:

$$p_j = - \frac{g_j}{\left(\alpha + \sum_{i=1}^j g_i\right) \left(\alpha + \sum_{i=1}^{j-1} g_i\right)}. \quad (7)$$

If the inverse of the envelop function γ^{-1} exists then the inverse of the Prandtl-Ishlinskii hysteresis model can be expressed as:

$$x_p^{-1}(t) = \gamma^{-1} \left(\alpha^{-1} v_p(t) + \sum_{j=1}^n p_j H_{q_j}[v_p](t) \right), \quad (8)$$

where $\alpha^{-1} = 1/\alpha$ and n is the number of generalized play operators.

3.4 System identification

In this section, the identification of different parameters of the Prandtl-Ishlinskii hysteresis model as well as the linear dynamics of the considered nanopositioning system will be presented. The parameter values of the hysteresis model are used to construct the inverse Prandtl-Ishlinskii hysteresis model which will be employed as a feed-forward controller to compensate for hysteresis nonlinearity of the piezoelectric actuator.

First, the output response from the piezoelectric actuator is measured for the triangular input voltage signal of 40 V with a frequency of 10 Hz. The real-time data acquisition is performed with a frequency of 10 kHz. The measured input-output response will generate the hysteresis loop. Then, to identify the parameters of the Prandtl-Ishlinskii hysteresis model, nonlinear curve fitting problem is solved in least-squares sense. This minimization problem has been solved by using the nonlinear least-square optimization toolbox in MATLAB. The identified values of the parameters are presented in Table 1.

Table 1. Different parameters values of the considered system

Parameters	Values
Identified parameter values	
c_0	0.3648
c_1	-0.1353
β	0.0570
ρ	2.1154
τ	9.1154
α	0.1801
n	20
Theoretical values	
G_v	10
ω_v	3 kHz
G_a	0.3 $\mu\text{m/V}$
ω_a	2100 Hz
G_c	0.3 $\text{V}/\mu\text{m}$
ω_c	10 kHz

The linear dynamics of the considered nanopositioning system is also identified experimentally. For this purpose,

sinusoidal input of increasing frequency (chirp signal) and small amplitude (so that hysteresis effects are negligible) is applied to the experimental platform. A recursive least square (RLS) parameter adaptation algorithm is used to minimize the prediction error between the system output and the output predicted by the model at each sampling instant. The identified 4th order transfer function of the considered nanopositioning system is given as follows:

$$G(s) = \frac{g_1 s^3 + g_2 s^2 + g_3 s + g_4}{s^4 + g_5 s^3 + g_6 s^2 + g_7 s + g_8}, \quad (9)$$

where $g_1 = 5095$, $g_2 = 1.2 \times 10^8$, $g_3 = 7 \times 10^{11}$, $g_4 = 4.65 \times 10^{15}$, $g_5 = 9501$, $g_6 = 2.44 \times 10^8$, $g_7 = 1.3 \times 10^{12}$ and $g_8 = 5.2 \times 10^{15}$.

The measured output as well as the output of the identified linear dynamics $G(s)$ is shown in Fig. 4 which shows the good match between the two plots. The minor difference between the two plots will be dealt with the robustness of the proposed feedback controllers.

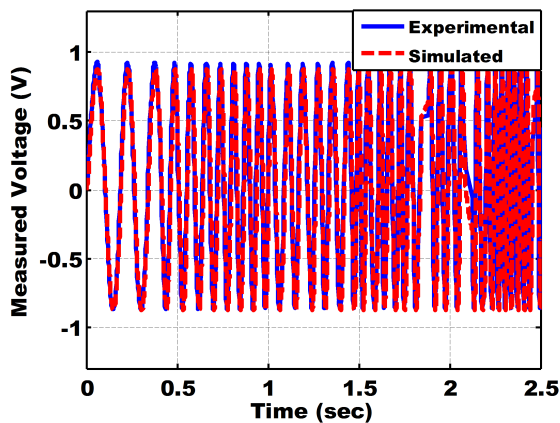


Fig. 4. Experimental and simulated responses of chirp input

The output of the Prandtl-Ishlinskii hysteresis model coupled with identified transfer function $G(s)$ will generate the hysteresis loop as shown in Fig. 5(a) (dotted line). Fig. 5(a) shows that the hysteresis loop in simulation acceptably fits with the measured hysteresis loop. The output response of inverse estimated Prandtl-Ishlinskii hysteresis model based on identified parameters (Table 1) for a triangle input voltage of amplitude 40 V and frequency of 10 Hz is shown in Fig. 5(b).

The inverse estimated Prandtl-Ishlinskii hysteresis model is used as a feed-forward compensator to mitigate hysteresis effects of piezoelectric actuator. Figure 6 shows the capability of the inverse model to compensate hysteresis effects in simulation. Figure 6 shows that that hysteresis effect has been compensated perfectly in simulation.

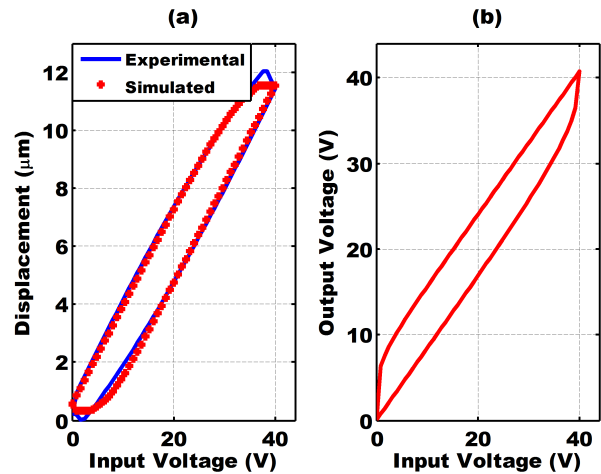


Fig. 5. (a) Experimental and simulated hysteresis loops with a triangle input voltage of amplitude 40 V and frequency of 10 Hz (b) Output response of the inverse estimated Prandtl-Ishlinskii hysteresis model

However, when same feed-forward compensator is implemented for real time experimentation, slight hysteresis nonlinearity still observed due to small mismatch between the output of identified hysteresis model and the measured hysteresis loop (see Section 5). To further enhance the performance of the piezoelectric actuator in terms of mitigation of hysteresis nonlinearity and precise reference tracking, advanced robust H_∞ feedback controllers (full-order and fixed-order) in the presence of feed-forward compensator are proposed and thoroughly analyzed here in this paper.

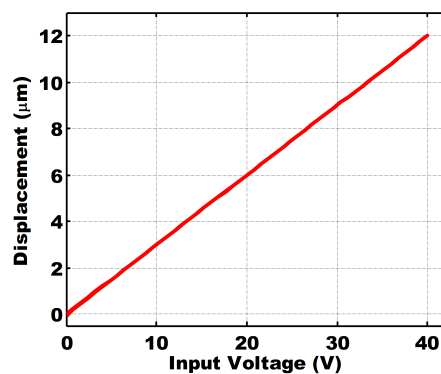


Fig. 6. Simulation result with inverse estimated Prandtl-Ishlinskii hysteresis model as a feed-forward compensator

4 H_∞ CONTROLLER DESIGN

After designing feed-forward compensator to mitigate hysteresis effects, now an H_∞ feedback controller $K(s)$

will be proposed for the linear dynamics $G(s)$ in order to achieve better reference tracking performance. Following two different H_{∞} feedback controllers will be analyzed here in this paper:

- Full-order H_{∞} controller
- Fixed-order H_{∞} controller

The important steps in designing H_{∞} feedback controller are the desired performance specification, selection of weighting functions and the creation of generalized plant model. These steps are discussed in the coming subsections.

4.1 Desired performance and sensitivity functions

The closed-loop sensitivity functions are classically given by following relations:

$$S(s) = \frac{1}{1 + G(s)K(s)}, \tag{10}$$

$$T(s) = \frac{G(s)K(s)}{1 + G(s)K(s)}, \tag{11}$$

where $S(s)$ and $T(s)$ are output and complementary sensitivity functions respectively, $G(s)$ is transfer function of the system and $K(s)$ is controller transfer function.

The desired performance of the considered system is to achieve a reference tracking error (peak-to-peak) of less than 1% for the desired displacement of 12 μm and frequency of 10 Hz with good robustness and stability margins. In order to have good robustness margin (which implies good stability margin), following conditions must be satisfied: $\|S(s)\|_{\infty} < 6$ dB and $\|T(s)\|_{\infty} < 3.5$ dB. This desired performance is imposed on the closed-loop sensitivity functions by using appropriate weighting functions.

4.2 Selection of weighting functions

Two weighting function $W_1(s)$ and $W_2(s)$ have been chosen here for the design of H_{∞} feedback controller. These functions weight the controlled outputs y_1 and y_2 as shown in Fig. 7 and are designed according to the desired performance requirements.

The transfer functions of the proposed weighting functions are as follows:

$$W_1(s) = \frac{0.5s + 2450}{s + 0.4901}, \tag{12}$$

$$W_2(s) = \frac{s + 4608}{0.05s + 6912}. \tag{13}$$

Here $W_1(s)$ is used to impose the desired performance specifications on closed-loop output sensitivity function $S(s)$ in terms of small tracking error, large bandwidth and

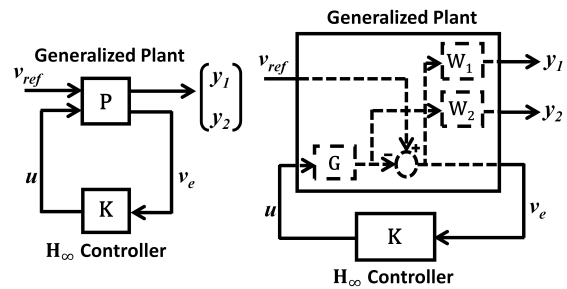


Fig. 7. Generalized plant (P) with controller (K) in H_{∞} framework

good robustness margin (i.e. $\|S(s)\|_{\infty} < 6$ dB). $W_2(s)$ is designed to impose limitations on complementary sensitivity function $T(s)$ in terms of good reference tracking, better attenuation of high frequency noise and good robustness margin (i.e. $\|T(s)\|_{\infty} < 3.5$ dB).

4.3 Generalized plant

The generalized plant P (i.e. the interconnection of the plant and weighting functions) as shown in Fig. 7 is given as follows:

$$\begin{bmatrix} y_1 \\ y_2 \\ v_e \end{bmatrix} = \underbrace{\begin{bmatrix} W_1 & -G \\ 0 & W_2 G \\ 1 & -G \end{bmatrix}}_P \begin{bmatrix} v_{ref} \\ u \end{bmatrix}. \tag{14}$$

The linear fractional transformation $F_l(P,K)$ is given by:

$$F_l(P, K) = \begin{bmatrix} W_1 S \\ W_2 T \end{bmatrix}, \tag{15}$$

where S and T are output and complementary sensitivity functions respectively and W_1 and W_2 are two weighting functions.

The objective of standard H_{∞} optimal control is to find a stabilizing controller $K(s)$ that minimizes the following [31]:

$$\|F_l(P, K)\|_{\infty} = \max_{\omega} \bar{\sigma}(F_l(P, K)(j\omega)), \tag{16}$$

where $\bar{\sigma}$ denotes the maximum singular value.

4.4 Full-order H_{∞} controller

The order of the full-order H_{∞} controller $K(s)$ will be the same as the order of the generalized plant model $P(s)$, hence the choice of the weighting functions is an important issue in the H_{∞} control problem.

The minimization problem of $\|F_l(P, K)\|_{\infty}$ in order to find a stabilizing full-order H_{∞} controller $K(s)$ is solved

by using the function, hinfsyn in MATLAB. The achieved minimum value of $\|F_l(P, K)\|_\infty$ over all possible stabilizing controllers K is 0.84. As achieved value is less than one, it means that the closed-loop sensitivity functions will remain below the inverse of corresponding weighting functions in all frequency range and accordingly all performance objectives will be achieved.

The following sixth order controller transfer function K(s) was obtained:

$$K(s) = \frac{n_1 s^5 + n_2 s^4 + n_3 s^3 + n_4 s^2 + n_5 s + n_6}{s^6 + d_1 s^5 + d_2 s^4 + d_3 s^3 + d_4 s^2 + d_5 s + d_6}, \tag{17}$$

where $n_1 = 3.2 \times 10^9$, $n_2 = 4.7 \times 10^{14}$, $n_3 = 4.9 \times 10^{18}$, $n_4 = 1.1 \times 10^{23}$, $n_5 = 5.9 \times 10^{26}$, $n_6 = 2.3 \times 10^{30}$, $d_1 = 8.2 \times 10^8$, $d_2 = 4.9 \times 10^{14}$, $d_3 = 1.1 \times 10^{19}$, $d_4 = 6.5 \times 10^{22}$, $d_5 = 4.3 \times 10^{26}$ and $d_6 = 1.4 \times 10^{26}$.

4.5 Fixed-order H_∞ controller

Other than full-order H_∞ feedback controller, fixed-order H_∞ controller is also designed here to analyze the performance of piezoelectric actuator system. Designing a fixed-order H_∞ controller where the order of the controller is fixed to be less than that of the open-loop plant, is a difficult, nonconvex and typically nonsmooth (nondifferentiable) optimization problem [32]. This optimization problem is solved by using the HIFOO (H-Infinity Fixed Order Optimization) toolbox [33].

HIFOO uses a hybrid algorithm for nonsmooth, nonconvex optimization in order to find a fixed-order controller with minimum closed-loop H_∞ norm [34]. The controller order is fixed *a priori* to be less than the order of the plant. HIFOO has been successfully applied for different applications in order to achieve a fixed-order H_∞ controller [35–37]. For our considered piezoelectric actuator system, the achieved minimum value of closed-loop H_∞ norm with HIFOO algorithm is 0.99. The closed-loop sensitivity functions with HIFOO will remain below the inverse of corresponding weighting functions in all frequency range as the achieved value of closed-loop H_∞ norm is less than unity.

The following third order controller transfer function K(s) was obtained:

$$K(s) = \frac{k_1 s^3 + k_2 s^2 + k_3 s + k_4}{s^3 + k_5 s^2 + k_6 s + k_7}, \tag{18}$$

where $k_1 = 1.3$, $k_2 = 5 \times 10^9$, $k_3 = 7.9 \times 10^{13}$, $k_4 = 1.6 \times 10^{18}$, $k_5 = 9.6 \times 10^8$, $k_6 = 4.3 \times 10^{14}$ and $k_7 = 1.7 \times 10^{14}$.

4.6 Closed-loop sensitivity functions

In this subsection, the closed-loop sensitivity functions (S and T) with both full-order and fixed-order (HIFOO) H_∞ controllers will be presented.

Figure 8 shows that the considered closed loop sensitivity functions (S and T) with both full-order and fixed-order H_∞ controllers remain below the inverse of the corresponding weighting functions in all frequency range. This will ensure good reference tracking performance with stability and robustness margins. With full-order H_∞ controller, the achieved gain margin is ∞, phase margin is 91.5°, $\|S\|_\infty = 0.1$ dB and $\|T\|_\infty = 0$ dB. With fixed-order H_∞ controller, the achieved gain margin is ∞, phase margin is 76.7°, $\|S\|_\infty = 0.6$ dB and $\|T\|_\infty = 0$ dB. It can be observed from Fig. 8(a) that the output sensitivity function (S) provides more attenuation at low frequency with full-order H_∞ controller as compared to fixed-order H_∞ controller. That is why less tracking error is expected with full-order H_∞ controller than with fixed-order H_∞ controller.

The tracking performance of the proposed controllers will be validated through real-time experimentation.

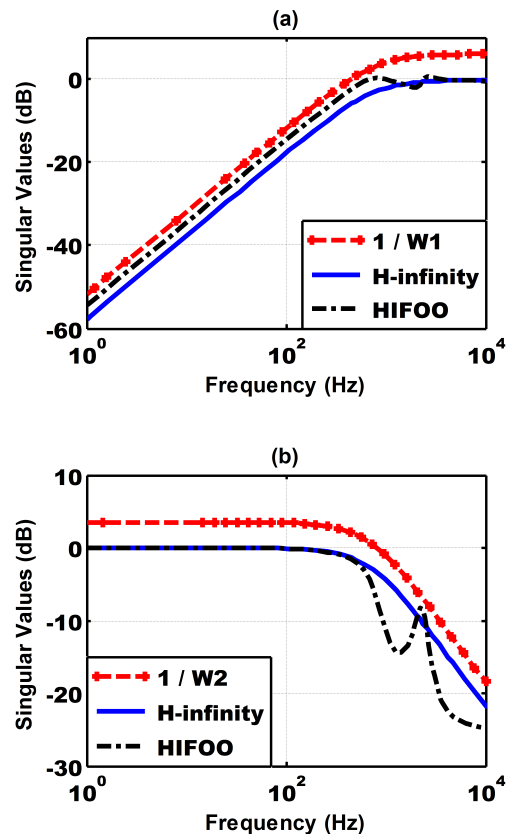


Fig. 8. (a) Magnitude response of output sensitivity function S and weighting function 1/W₁ (b) Magnitude response of complimentary sensitivity function T and weighting function 1/W₂

5 EXPERIMENTAL RESULTS

In this section, open-loop (without any compensator and with a feed-forward compensator) as well as closed-loop (with full-order and fixed-order H_∞ feedback controllers in the presence of a feed-forward compensator) experimental results of hysteresis compensation and reference tracking error will be presented.

5.1 Hysteresis compensation

Figure 9 shows the experimental result of hysteresis loop in open loop without any compensator. Output displacement of the piezoelectric actuator with large hysteresis loop can be observed (hysteresis percentage of 24.38%).

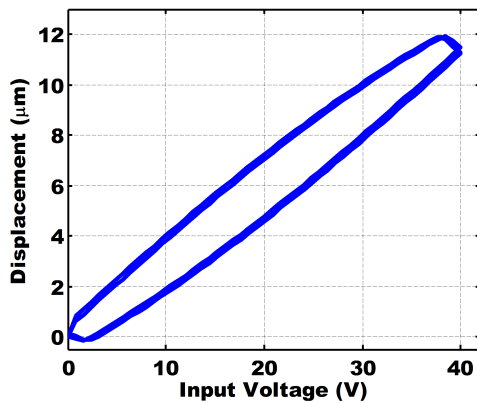


Fig. 9. Experimental result of hysteresis loop in open-loop without compensation

Figure 10 shows the experimental result when inverse estimated Prandtl-Ishlinskii hysteresis model is used as a feed-forward compensator. We can observe slight hysteresis nonlinearity (hysteresis percentage of 3.63%) in the output displacement that is not compensated by the inverse model. This hysteresis yields error in the output displacement which is due to fact that the identified hysteresis model is an approximation of the measured hysteresis loop.

Figure 11 and Fig. 12 shows the experimental results when full-order and fixed-order H_∞ feedback controllers are used in the presence of feed-forward compensator. These feedback controllers with inverse estimated Prandtl-Ishlinskii hysteresis model show better compensation of hysteresis nonlinearities of piezoelectric actuator as compared to open-loop compensation with a feed-forward compensator. Hysteresis percentage of 0.96% is achieved with full-order H_∞ feedback controller and 1.34% with fixed-order H_∞ feedback controller.

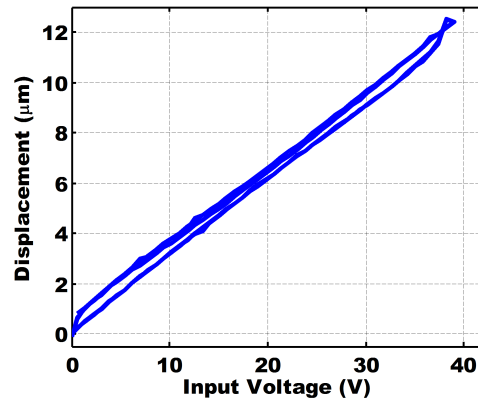


Fig. 10. Experimental result of hysteresis loop in open-loop with feed-forward compensator

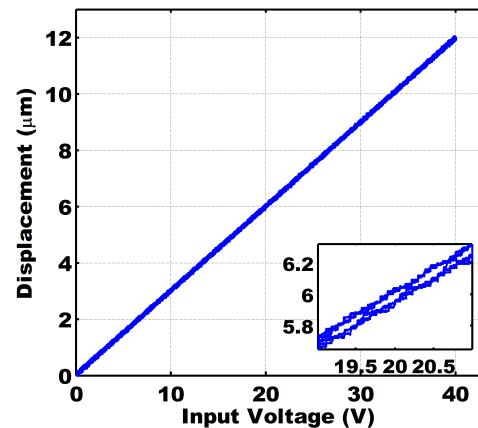


Fig. 11. Experimental result of hysteresis loop in closed-loop with full-order H_∞ feedback controller in the presence of feed-forward compensator

5.2 Reference tracking error

In this subsection, the experimental results of peak-to-peak tracking error with desired triangular displacement of $12 \mu\text{m}$ with frequency of 10 Hz are presented. The presented tracking error plots in this subsection are the difference between the reference and process value.

Figure 13 shows the open-loop reference tracking error without any compensator. The observed peak-to-peak tracking error is $2.66 \mu\text{m}$ which is 22.17% of the desired displacement of piezoelectric actuator.

Figure 14 shows the open-loop reference tracking error when inverse estimated Prandtl-Ishlinskii hysteresis model is used as a feed-forward compensator. The observed peak-to-peak tracking error is $1.36 \mu\text{m}$ now which is 11.33% of the desired displacement of piezoelectric actuator.

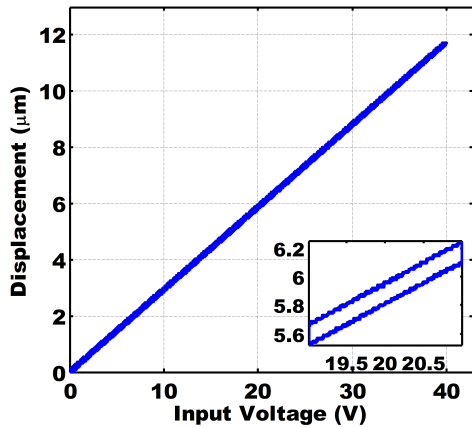


Fig. 12. Experimental result of hysteresis loop in closed-loop with fixed-order H_∞ feedback controller (HIFOO) in the presence of feed-forward compensator

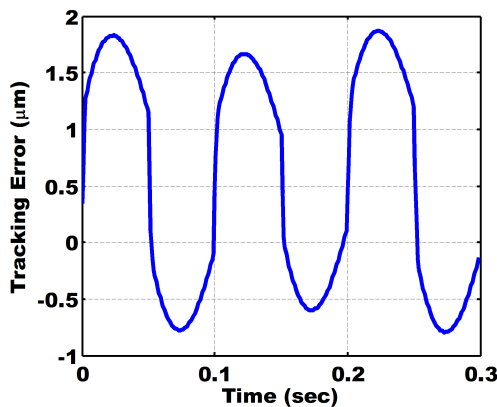


Fig. 13. Experimental result of tracking error in open-loop without compensation

Finally, the reference tracking error plots with proposed full-order and fixed-order H_∞ feedback controllers in the presence of feed-forward compensator are presented in Fig. 15 and Fig. 16 respectively. Here, the achieved peak-to-peak tracking errors with full-order H_∞ feedback controller is 0.09 μm (0.75% of the desired displacement) and with fixed-order H_∞ feedback controller it is 0.37 μm (3.08% of the desired displacement). These results show the capability of the H_∞ controller with inverse Prandtl-Ishlinskii hysteresis model to compensate effectively the hysteresis effects of the piezoelectric actuator.

Overall, the performance comparison has been summarized in Table 2.

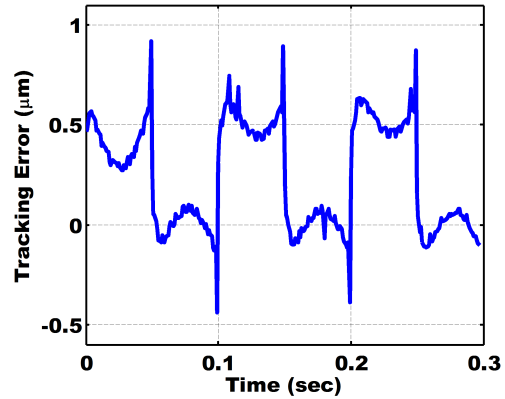


Fig. 14. Experimental result of tracking error in open-loop with feed-forward compensator

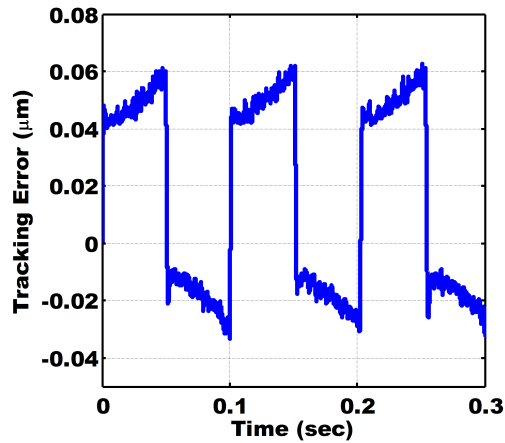


Fig. 15. Experimental result of tracking error in closed-loop with full-order H_∞ feedback controller in the presence of feed-forward compensator

6 CONCLUSION

In this paper, nonlinear hysteresis effect of the considered piezoelectric actuator has been characterized using the Prandtl-Ishlinskii hysteresis model. Different parameters of the hysteresis model as well as the linear dynamics of the considered system have been identified from the real-time experimental data. Then, inverse Prandtl-Ishlinskii hysteresis model has been used as a feed-forward controller to compensate the hysteresis effects of the considered piezoelectric actuator system. Still, 3.63% of hysteresis with 11.33% of peak-to-peak tracking error has been observed. To further enhance the performance of the considered piezoelectric actuator system, advanced robust full-order as well as fixed-order H_∞ feedback controllers have been analyzed in the presence of feed-forward com-

Table 2. Performance comparison

	Without Compensator	With Feed-Forward Compensator	With Fixed-Order H_∞ Controller	With Full-Order H_∞ Controller
Hysteresis	24.38%	3.63%	1.34%	0.96%
Peak-to-Peak Tracking Error	22.17%	11.33%	3.08%	0.75%

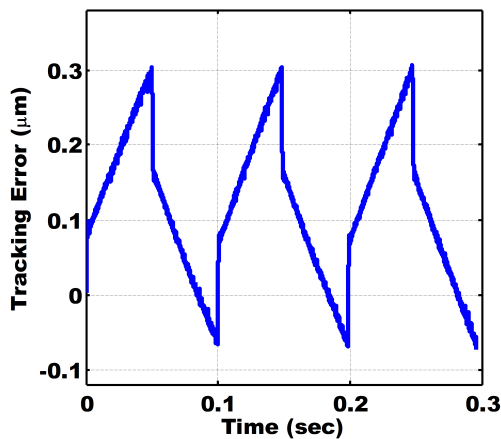


Fig. 16. Experimental result of tracking error in closed-loop with fixed-order H_∞ feedback controller (HIFOO) in the presence of feed-forward compensator

compensator. The achieved experimental results show that the proposed control scheme with both H_∞ feedback controllers can effectively suppress the hysteresis nonlinearities and accordingly can reduce the peak-to-peak tracking error. A better performance with full-order H_∞ feedback controller was achieved as compared to fixed-order H_∞ feedback controller. 0.96% of hysteresis with 0.75% of peak-to-peak tracking error has been achieved with full-order H_∞ feedback controller as compare to 1.34% of hysteresis with 3.08% of peak-to-peak tracking error with fixed-order H_∞ feedback controller. The experimental results show that the desired performance of peak-to-peak tracking error of less than 1% for the reference displacement of 12 μm with tracking frequency of 10 Hz has been achieved with full-order H_∞ feedback controller in the presence of feed-forward compensator.

ACKNOWLEDGMENT

The authors gratefully acknowledge the technical and financial support of Research Center of College of Engineering, Deanship of Scientific Research, King Saud University.

REFERENCES

- [1] S. Devasia, E. Eleftheriou, and S. R. Moheimani, "A survey of control issues in nanopositioning," *IEEE Transactions on Control Systems Technology*, vol. 15, no. 5, pp. 802–823, 2007.
- [2] G. Binnig and H. Rohrer, "Scanning tunneling microscopy," *IBM Journal of research and development*, vol. 44, no. 1/2, p. 279, 2000.
- [3] J.-C. Shen, W.-Y. Jywe, H.-K. Chiang, and Y.-L. Shu, "Precision tracking control of a piezoelectric-actuated system," *Precision Engineering*, vol. 32, no. 2, pp. 71–78, 2008.
- [4] T. Pare and J. P. How, "Robust stability and performance analysis of systems with hysteresis nonlinearities," in *IEEE American Control Conference*, vol. 3, pp. 1904–1908, 1998.
- [5] M. Brokate and J. Sprekels, *Hysteresis and phase transitions*, vol. 121. Springer Science & Business Media, 2012.
- [6] M. Ismail, F. Ikhouane, and J. Rodellar, "The hysteresis bouc-wen model, a survey," *Archives of Computational Methods in Engineering*, vol. 16, no. 2, pp. 161–188, 2009.
- [7] R. Ouyang and B. Jayawardhana, "Absolute stability analysis of linear systems with duhem hysteresis operator," *Automatica*, vol. 50, no. 7, pp. 1860–1866, 2014.
- [8] S. E. Zirka, Y. I. Moroz, R. G. Harrison, and K. Chwastek, "On physical aspects of the jiles-atherton hysteresis models," *Journal of Applied Physics*, vol. 112, no. 4, p. 043916, 2012.
- [9] P. Ge and M. Jouaneh, "Generalized preisach model for hysteresis nonlinearity of piezoceramic actuators," *Precision Engineering*, vol. 20, no. 2, pp. 99–111, 1997.
- [10] M. A. Krasnosel'skii and A. V. Pokrovskii, *Systems with hysteresis*. Springer Science & Business Media, 2012.
- [11] J. Gan, X. Zhang, and H. Wu, "A generalized prandtl-ishlinskii model for characterizing the rate-independent and rate-dependent hysteresis of piezoelectric actuators," *Review of Scientific Instruments*, vol. 87, no. 3, p. 035002, 2016.
- [12] Y. Liu, H. Liu, H. Wu, and D. Zou, "Modelling and compensation of hysteresis in piezoelectric actuators based on maxwell approach," *Electronics Letters*, vol. 52, no. 3, pp. 188–190, 2015.
- [13] M. Al Janaideh, J. Mao, S. Rakheja, W. Xie, and C.-Y. Su, "Generalized prandtl-ishlinskii hysteresis model: Hysteresis modeling and its inverse for compensation in smart actuators," in *IEEE Conference on Decision and Control*, pp. 5182–5187, 2008.

- [14] M. Al Janaideh, M. Rakotondrabe, and O. Aljanaideh, "Further results on hysteresis compensation of smart micropositioning systems with the inverse prandtl–ishlinskii compensator," *IEEE Transactions on Control Systems Technology*, vol. 24, no. 2, pp. 428–439, 2016.
- [15] M. Al Janaideh, R. Naldi, L. Marconi, and P. Krejčí, "A hybrid system for a class of hysteresis nonlinearity: modeling and compensation," in *IEEE Conference on Decision and Control*, pp. 5380–5385, 2012.
- [16] M. Rakotondrabe, Y. Haddab, and P. Lutz, "Quadrilateral modelling and robust control of a nonlinear piezoelectric cantilever," *IEEE Transactions on Control Systems Technology*, vol. 17, no. 3, pp. 528–539, 2009.
- [17] A. Esbrook, X. Tan, and H. K. Khalil, "Inversion-free stabilization and regulation of systems with hysteresis via integral action," *Automatica*, vol. 50, no. 4, pp. 1017–1025, 2014.
- [18] W.-F. Xie, J. Fu, H. Yao, and C.-Y. Su, "Neural network-based adaptive control of piezoelectric actuators with unknown hysteresis," *International Journal of Adaptive Control and Signal Processing*, vol. 23, no. 1, pp. 30–54, 2009.
- [19] M. Al Janaideh and D. S. Bernstein, "Inversion-free adaptive control of uncertain systems with shape-memory-alloy actuation," in *IEEE American Control Conference*, pp. 3579–3584, 2013.
- [20] L. Riccardi, D. Naso, B. Turchiano, and H. Janocha, "Design of linear feedback controllers for dynamic systems with hysteresis," *IEEE Transactions on Control Systems Technology*, vol. 22, no. 4, pp. 1268–1280, 2014.
- [21] B. Bhikkaji, M. Ratnam, A. J. Fleming, and S. R. Moheimani, "High-performance control of piezoelectric tube scanners," *IEEE Transactions on Control Systems Technology*, vol. 15, no. 5, pp. 853–866, 2007.
- [22] A. J. Fleming, "A method for reducing piezoelectric nonlinearity in scanning probe microscope images," in *IEEE American Control Conference*, pp. 2861–2866, 2011.
- [23] M. Ruderman and T. Bertram, "Control of magnetic shape memory actuators using observer-based inverse hysteresis approach," *IEEE Transactions on Control Systems Technology*, vol. 22, no. 3, pp. 1181–1189, 2014.
- [24] K. Seki, M. Ruderman, and M. Iwasaki, "Modeling and compensation for hysteresis properties in piezoelectric actuators," in *IEEE 13th International Workshop on Advanced Motion Control (AMC)*, pp. 687–692, 2014.
- [25] Y. Liu, J. Shan, and U. Gabbert, "Feedback/feedforward control of hysteresis-compensated piezoelectric actuators for high-speed scanning applications," *Smart Materials and Structures*, vol. 24, no. 1, p. 015012, 2014.
- [26] K. K. Leang and S. Devasia, "Feedback-linearized inverse feedforward for creep, hysteresis, and vibration compensation in afm piezoactuators," *IEEE Transactions on Control Systems Technology*, vol. 15, no. 5, pp. 927–935, 2007.
- [27] S. Salapaka, A. Sebastian, J. P. Cleveland, and M. V. Salapaka, "High bandwidth nano-positioner: A robust control approach," *Review of scientific instruments*, vol. 73, no. 9, pp. 3232–3241, 2002.
- [28] A. Sebastian and S. M. Salapaka, "Design methodologies for robust nano-positioning," *IEEE Transactions on Control Systems Technology*, vol. 13, no. 6, pp. 868–876, 2005.
- [29] I. Ahmad, A. Voda, and G. Besançon, "Robust h-infinity control of a scanning tunneling microscope under parametric uncertainties," in *IEEE American Control Conference*, pp. 6555–6560, 2010.
- [30] I. Ahmad, A. Voda, G. Besançon, and G. Buche, "Tunneling current analysis over an experimental platform with h-infinity control," *Journal European des Systemes Automatises*, vol. 4, pp. 507–534, 2012.
- [31] S. Skogestad and I. Postlethwaite, *Multivariable feedback control: analysis and design*, vol. 2. Wiley New York, 2007.
- [32] J. Burke, D. Henrion, A. Lewis, and M. Overton, "Hifoo—a matlab package for fixed-order controller design and h-infinity optimization," in *Fifth IFAC Symposium on Robust Control Design, Toulouse*, 2006.
- [33] S. Gumussoy, D. Henrion, M. Millstone, and M. L. Overton, "Multiobjective robust control with hifoo 2.0," *IFAC Proceedings Volumes*, vol. 42, no. 6, pp. 144–149, 2009.
- [34] S. Gumussoy and M. L. Overton, "Fixed-order h-infinity controller design via hifoo, a specialized nonsmooth optimization package," in *Proceedings of the 2008 American Control Conference*, pp. 2750–2754, 2008.
- [35] S. Türkay and H. Akçay, "Multi-objective control of full-vehicle suspensions: A case study," *IFAC Proceedings Volumes*, vol. 44, no. 1, pp. 1826–1831, 2011.
- [36] G. Puyou and P. Ezerzere, "Tolerance of aircraft longitudinal control to the loss of scheduling information: toward a performance oriented approach," *IFAC Proceedings Volumes*, vol. 45, no. 13, pp. 393–399, 2012.
- [37] M. Řezáč and Z. Hurák, "Structured mimo h-infinity design for dual-stage inertial stabilization: Case study for hifoo and hinfstruct solvers," *Mechatronics*, vol. 23, no. 8, pp. 1084–1093, 2013.



Irfan Ahmad received the M.Sc. and Ph.D. degrees in Control Systems from University of Grenoble (INPG), France in 2007 and 2011 respectively. He is currently an assistant professor in electrical engineering department of King Saud University where he is also the member of Automation and Intelligent Systems research group. His current research interests include optimal and robust control design for micro/nanopositioning systems and for UAVs.



Akram M. Abdurraqeab received the B.Sc. degree in Electrical Engineering from Taiz University, Yemen in 2008. He is currently completing his master's thesis in Automatic Control from electrical engineering department of King Saud University. His research interests include application of robust control for micro/nanopositioning systems, robotics and renewable energy.

AUTHORS' ADDRESSES

Irfan Ahmad, Ph.D.

Akram M. Abdurraqeab, M.Sc.

Electrical Engineering Department,

College of Engineering,

King Saud University,

P.O. Box 800, SA-11421 Riyadh, Saudi Arabia

email: irfahmad@ksu.edu.sa, encom.akram@gmail.com

Received: 2016-05-05

Accepted: 2016-11-05